FMCW Ramp Non-Linearity Effects and Measurement Technique for Cooperative Radar

Andreas Frischen*, Juergen Hasch*, and Christian Waldschmidt†
*Robert Bosch GmbH, Corporate Sector Research and Advance Engineering, P.O. Box 10 60 50, 70049 Stuttgart, Germany
†Institute of Microwave Techniques, Ulm University, Albert-Einstein-Allee 41, 89081 Ulm, Germany
Email: {andreas.frischen, juergen.hasch}@de.bosch.com, christian.waldschmidt@uni-ulm.de

***Abstract*—In FMCW radars, the linearity of the generated ramp has a determining influence on the range resolution and accuracy. This is especially true for cooperative radar systems, where the ramps for modulation and down-conversion are generated separately, strongly increasing the impact of ramp non-linearities. In this paper, the causes for ramp non-linearities in a PLL-based synthesizer are discussed and modeled as phase deviations from an ideal ramp. A measurement technique to determine these deviations is introduced, where both the hardware setup and the necessary digital processing steps are presented. It is exemplarily applied to an FMCW synthesizer with an integrated 122-GHz transceiver, evaluating the influences of PLL parameters on ramp linearity. Reference measurements show that phase deviations in the low mrad range can be determined with this technique.**

I. Introduction

Frequency-modulated continuous wave (FMCW) and derived schemes currently constitute the dominant modulation for civil radar applications. Non-linearities of the FMCW ramp reduce the achievable range resolution and accuracy, as they lead to a broadened peak in the baseband spectrum. A quantitative study of this effect has been published in [1].

In a conventional homodyne monostatic radar, the received target response is mixed with the same signal that was transmitted to generate the target response. Due to this correlation, the effects of phase noise and ramp non-linearities are diminished for short flight times of the transmit signal. Particularly, the remaining performance degradation arises from the varying slope. Additionally, techniques to reduce the effects of ramp non-linearities exist [2], [3]. In contrast, the transmitted modulated signal and the signal for downconversion are generated independently in a cooperative bistatic radar sensor system. Thus, not only the varying slope, but also slowly-varying frequency offsets result in perturbation of the downconverted received signal and have an impact on the performance in terms of range resolution and accuracy. A measurement technique for the evaluation of ramp linearity in a cooperative radar should therefore regard any deviations from an ideal ramp.

A common method is the evaluation of the radar baseband signal in a setup with a single simulated target, where the varying slope can be analyzed. The instantaneous frequency and phase offset to the ideal ramp, however, can only be determined by integration, which leads to large phase errors. Another method is the wide-band observation of the modulated RF signal after a frequency divider e.g. in a real-time spectrum analyzer. However, high-precision phase measurements require a high-resolution signal acquisition, while high sampling rates generally reduce the attainable resolution.

The proposed method of this work relies on the narrow-band observation of the divided RF signal by mixing it with an approximately ideal linear frequency ramp with the same parameters and a small frequency offset. By sampling and suitable processing of this low-frequency signal, the phase deviations from an ideal ramp are evaluated. The technique is applied to an FMCW frequency synthesizer with an integrated 122-GHz transceiver [4] and a commercially available phase locked loop (PLL) chip incorporating a phase frequency detector (PFD), a charge pump, and modulation capabilities. The PLL-internal modulation technique based on stepwise changing of the divider value entails non-linearities that are discussed in section II-B and evaluated in section IV.

II. Signal Model

A. Bistatic Signal Model

In a cooperative MIMO radar with M distributed radar sensors, individual signal generation is performed at each sensor position. The aim of such a system design is either to measure the distances between the two active stations or to exploit the spatial diversity with widely separated antennas to improve object detection. In the first case, only one distance is measured and the use of the second station instead of a passive reflector improves the applicability in environments with large metallic objects [5]. In the latter case, the bistatic distances from a sensor m to the target to a different sensor n are estimated, in addition to the monostatic distances from every sensor position to the target, thus realizing a MIMO radar with separated stations. Here, the processing of the bistatic part is more critical, as phase noise and non-linearities occur independently on transmitter and receiver side with the result that they do not correlate. Fig. 1 illustrates the overall setup and the system design with signal paths for the signal transmitted at station 1. The paths of the other transmitted signals are omitted for reasons of clarity. A signal processing technique for the bistatic response has been published in [6]. The underlying signal model for the cooperative MIMO radar with distributed stations is shortly recapitulated in the following.

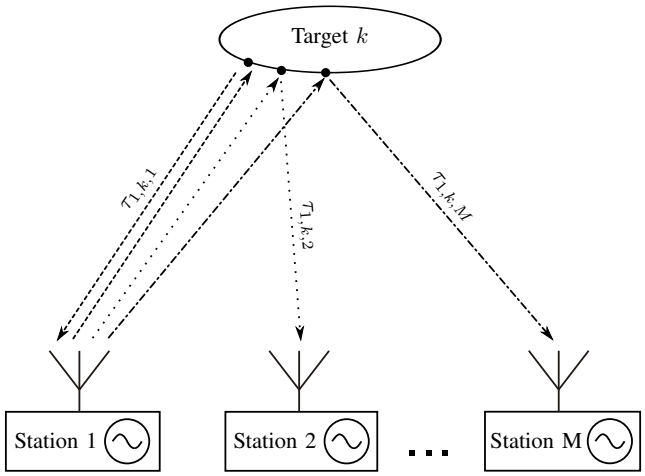

Fig. 1. Signal paths for the signal transmitted at station 1

The FMCW transmit signal of station $m, m \in \{1 \dots M\}$ at position $p_m \in \mathbb{R}^3$ is given by

$$s_m(t) = A_m \cdot \exp\left(j\big(2\pi f_m t + \pi k_r t^2 + \theta_m + \phi_m(t)\big)\right) \quad (1)$$

with the amplitude A_m, a constant start phase θ_m, the fundamental frequency f_m and the slope $k_r = \frac{f_{\mathrm{mod}}}{T_{\mathrm{mod}}}$, where f_{mod} represents the bandwidth and T_{mod} the modulation time of the ramp. The term $\phi_m(t)$ accounts for time-variant phase deviations from the ideal ramp and can be regarded as ramp non-linearities in the broader sense.

The received signal is composed of the sum of all transmitted and reflected signals at all K targets.

$$r_m(t) = \sum_{k=1}^{K} \sum_{n=1}^{M} a_{n,k,m} \cdot s_n\left(t - \tau_{n,k,m}\right) \quad (2)$$

Here, $a_{n,k,m}$ and $\tau_{n,k,m}$ describe the attenuation and travel time from station n to the reflection point on the surface of target k and further to station m, respectively. Subsequently, the received signal is downconverted to an intermediate frequency (IF) by mixing with the transmit signal of station m.

$$\begin{aligned} r_{m,\mathrm{bb}}(t) &= r_m^*(t) s_m(t) \\ &= A_m \cdot \sum_{k=1}^{K} \sum_{n=1}^{M} A_n \cdot a_{n,k,m} \exp\Big(j\big(2\pi(f_m - f_n)t \\ &\quad + 2\pi f_n \tau_{n,k,m} + 2\pi k_r \tau_{n,k,m} t - \pi k_r \tau_{n,k,m}^2 \\ &\quad + \theta_m - \theta_n + \phi_m(t) - \phi_n(t - \tau_{n,k,m})\big)\Big) \end{aligned} \quad (3)$$

The effective phase deviation in the received IF signal is therefore comprised of a constant part $\theta_m - \theta_n$ and the perturbation $\phi_m(t) - \phi_n(t - \tau_{n,k,m})$, where the latter causes a degradation in distance estimation performance.

B. Phase Deviation Model

In [1], the non-linearities in the FMCW ramp have been modeled in the received IF signal as a phase modulation with a sum of cosines. This leads to sidebands shifted by the respective modulation frequency and amplitudes according to the Bessel functions of the first kind of the respective modulation index. However, it describes only the effects of one specific systematic non-linearity. A more general approach is the following statistical description of phase deviations, that can be quantified by measurements.

In a cooperative radar, different causes can lead to the phase deviation $\phi_m(t)$ and consequently to a broadened target peak in the baseband spectrum.

1) Phase noise
2) Constant slope offset
3) Ramp non-linearities

First, phase noise leads to reciprocal mixing in the presence of close interferers or other targets. While it is also of concern for monostatic radars, the influence is even more significant for cooperative bistatic radars due to the missing correlation of the phase noise generated in the frequency synthesizers of the transmitting and receiving stations [7]. Second, a slightly different ramp slope at the two involved stations leads to a linearly time-varying offset frequency, which directly affects all target responses in the baseband spectrum. In contrast, a constant frequency offset shifts all target responses and is compensated by the signal processing technique in [6]. Third, the frequency modulation contains non-linearities depending on the architecture of the frequency synthesizer. In commercial radar applications, a PLL with fractional divider is commonly used for this purpose. Here, the frequency ramp is generated by constantly changing the divider value in the feedback loop. For the interval between two changes, the generated frequency would remain constant, if the bandwidth of the control loop was sufficiently high. As this behavior is unwanted, the rate at which the divider value changes has to be chosen smaller than the loop filter cutoff frequency. Nevertheless, a deviation from the ideally linear frequency modulation remains. All three effects are represented in the total phase deviation $\phi_m(t)$, that can be assessed with the measurement technique in section III.

The standard deviation $\sigma_{\mathrm{pd,m}}$ of the phase deviation $\phi_m(t)$ during the modulation time of the ramp can be used as a figure of merit of the linearity. Using this formulation, the correlation of the phase fluctuations over time is not regarded. While this negelct may seem to be unrealistic at first glance, the applicability of the model on cooperative radar systems is not effected, where correlation is performed between two independent signal sources, resulting in the term $\phi_{0,m}(t) - \phi_{0,n}(t - \tau_{n,k,m})$ in (3). In contrast, the effective phase deviation in a monostatic homodyne radar depends on $\phi_{0,m}(t) - \phi_{0,m}(t - \tau_{n,k,m})$, strongly depending on the correlation of the phase deviations over time.

In total, the phase of the IF signal for a single target in (3) is perturbed by the superposition of the phase deviations of the frequency synthesizers in both stations.

$$\sigma_{\mathrm{pd,total}}^2 = \sigma_{\mathrm{pd,m}}^2 + \sigma_{\mathrm{pd,n}}^2. \quad (4)$$

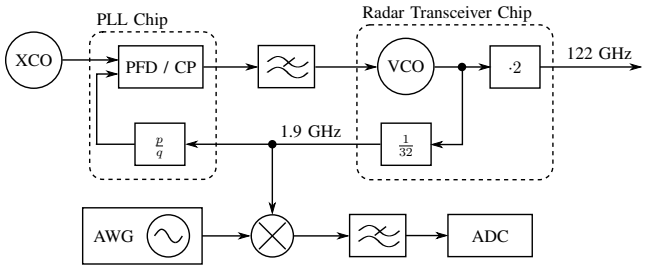

Fig. 2. Ramp linearity measurement setup with 122-GHz transceiver

III. Ramp Linearity Measurement

A. Hardware Setup

The proposed measurement principle is to mix the ramp that has been generated by the frequency synthesizer under test with a quasi-ideal reference ramp. Commonly, mm-wave transceivers integrate a frequency divider providing an output signal in the lower GHz range, that can be used for the ramp linearity measurements. This allows the use of arbitrary waveform generators (AWGs) as source for the reference ramp, since newer generations cover this frequency range and provide an excellence phase noise performance.

For the following measurements, the circuit under test consists of a commercially available modulating fractional-n PLL, a third order loop filter with cutoff frequency $f_\mathrm{c} = 300\,\mathrm{kHz}$ and an integrated 122-GHz transceiver chip. The latter comprises a 60-GHz push-push oscillator, a frequency doubler to provide the 122-GHz output frequency, and a divide-by-32 circuit as feedback for the PLL loop. The divided signal is in the range of $1.9\,\mathrm{GHz}$ and contains the same non-linearities and phase noise as the 122-GHz output scaled by a factor of $20\log(64)\,\mathrm{dB} = 36\,\mathrm{dB}$. The frequency ramp is generated by altering the fractional divider value $\frac{p}{q}$ internally over time.

The reference ramp with identical ramp parameters regarding modulation time and bandwidth is generated by an AWG. The two ramps are mixed and the low-pass-filtered mixer output is sampled with rate $f_\mathrm{sample}^\mathrm{IF}$, obtaining a bandwidth of $f_\mathrm{bw}^\mathrm{IF} = \frac{1}{2} f_\mathrm{sample}^\mathrm{IF}$. Proper synchronization of both ramps is essential, as time differences lead to a frequency shift in the IF signal, whereas the offset frequency f_off must be within the obtained range, i.e. $f_\mathrm{off} < f_\mathrm{bw}^\mathrm{IF}$. However, predictable timing errors can be compensated by adjusting the start frequency of one of the ramps. By setting $f_\mathrm{off} = \frac{1}{2} f_\mathrm{bw}^\mathrm{IF}$, the two sidebands of the spectrum around f_off are acquired equally. The overall measurement setup is depicted in Fig. 2.

B. Signal Processing

The sampled IF signal contains the carrier signal with phase noise and deviations from the ideal ramp around the offset frequency f_off. The following steps are applied to extract the desired stochastic information:

1) Determine f_off by finding the carrier peak in the frequency domain
2) Generate the analytic signal with the Hilbert transform
3) Downconvert the analytic signal to baseband digitally by multiplication with $\exp(-j2\pi f_\mathrm{off} t)$
4) Limit the downconverted signal to the analyzed bandwidth $f_\mathrm{bw}^\mathrm{ana} < f_\mathrm{off}$ by lowpass-filtering
5) Calculate the phase perturbation towards the ideal ramp as the unwrapped angles of the analytic signal
6) Calculate the standard deviation $\sigma_\mathrm{pd,m}$ of the phase perturbation

In the first step, an interpolating technique such as zero padding of the input signal is necessary to achieve a sufficient precision. Otherwise, the observed phase deviations exhibit a trend over time. Step 4 is necessary to suppress the wrapped part of the spectrum after the downconversion in step 3. Assessing the overall phase deviation over time delivered by step 5, the valid time range can be determined, on which step 6 is evaluated.

TABLE I
Measurement Parameters

Parameter	Value	Description
$f_\mathrm{start}^\mathrm{divider}$	1.9125 GHz	Ramp start frequency at divider
$f_\mathrm{start}^\mathrm{divider} - f_\mathrm{start}^\mathrm{AWG}$	500 kHz	Offset frequency
$f_\mathrm{mod}^\mathrm{RF}$	500 MHz	RF modulation bandwidth
T_mod	1 ms	Modulation time
$f_\mathrm{sample}^\mathrm{AWG}$	25 GS/s	AWG sampling frequency
$f_\mathrm{sample}^\mathrm{IF}$	2 MS/s	IF sampling frequency

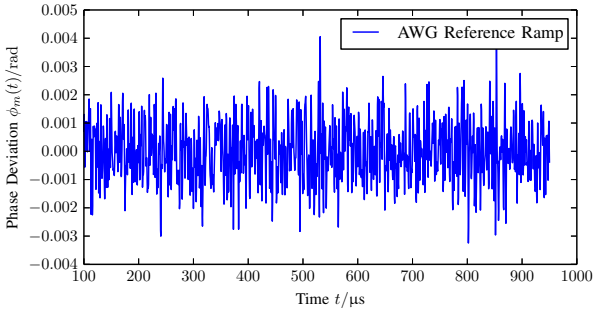

Fig. 3. Measured phase deviation for nearly-ideal AWG ramp

IV. Results

The phase deviations of a ramp generated by the circuit with a 122-GHz transceiver shown Fig. 2 was to be assessed. The parameters for this measurement are given in Tab. I.

Initially, the accuracy achievable with the setup was evaluated to ensure the validity of the measurements. Therefore, a ramp with the same parameters and signal level has been generated with the second channel of the AWG and the introduced processing was applied to this nearly-ideal ramp. The resulting measured phase deviation plotted in Fig. 3 shows an excellently narrow statistical phase distribution with $\sigma_\mathrm{pd}^\mathrm{AWG} \approx 1.0\,\mathrm{mrad}$. This value sets a lower bound for the quantifiable phase deviations measured with this technique.

The phase deviation of the 122-GHz transceiver ramp using 500 frequency steps in the PLL is plotted in Fig. 4 for

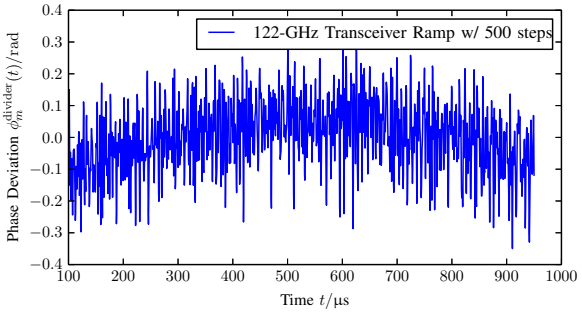

Fig. 4. Measured phase fluctuations of 122-GHz transceiver ramp with 500 frequency steps

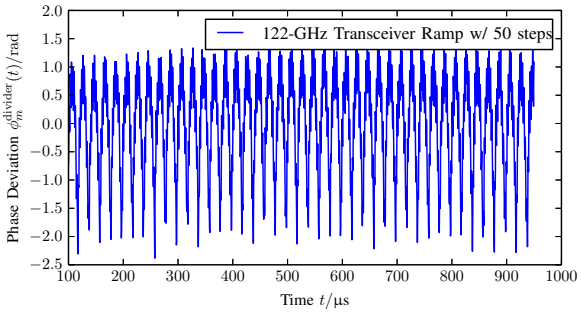

Fig. 5. Measured phase fluctuations of 122-GHz transceiver ramp with 50 frequency steps

the valid time range after transient effects $100\,\mu\text{s} < t < 950\,\mu\text{s}$. Here, the phase fluctuates with a standard deviation of $\sigma_{\text{pd}}^{\text{transceiver}} \approx 0.11\,\text{rad}$. It is dominated by phase noise, which is superimposed by a small parabolic function, due to a slight deviation of the ramp slope.

If the number of steps is smaller than the loop-filter cutoff frequency, strong non-linearities appear in the output of the synthesizer. Figure 5 shows the resulting phase fluctuations for 50 steps per ramp. Here, systematic non-linearities with a repetition interval equal to that of the frequency steps become apparent. The frequency spectrum around the modulated carrier of the generated ramp is depicted in Fig. 6. As predicted in the model in [1], spurs at multiples of the modulation step frequency of 50 kHz are present. For a large number of

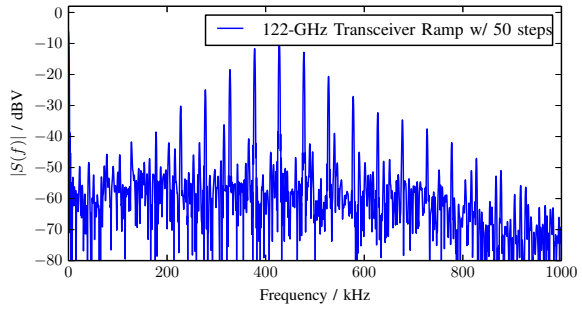

Fig. 6. Frequency spectrum around modulated carrier for 122-GHz transceiver ramp with 50 frequency steps

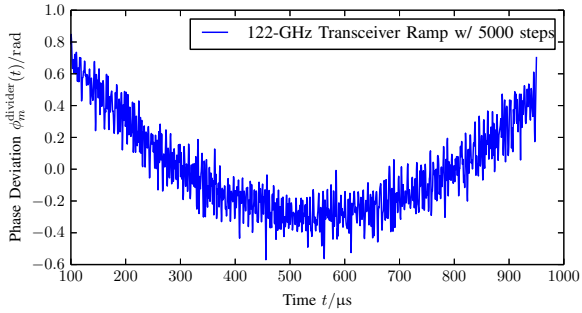

Fig. 7. Measured phase fluctuations of 122-GHz transceiver ramp with 5000 frequency steps

frequency steps, the step height becomes small and cannot be precisely adjusted. As a result, the slope deviates stronger from the ideal value and the parabolic function dominates the phase deviations. The measurement for an FMCW ramp with 5000 steps in Fig. 7 illustrates this behavior.

V. Conclusion

In this work, different causes for phase perturbations in the RF signal of a frequency synthesizer have been discussed. It has been demonstrated that the dimensioning of the frequency step width and height for the modulating PLL has a determining influence on the resulting linearity. A measurement technique has been presented that allows the evaluation of phase perturbations affecting the ramp linearity. The proposed method was applied to a circuit under test with a 122-GHz transceiver chip and a modulating PLL. Verified by reference measurements, phase perturbations in the low mrad range are measurable with the presented technique, which can be used to optimize the design of PLL-based frequency synthesizers.

References

[1] M. Pichler, A. Stelzer, P. Gulden, and M. Vossiek, "Influence of systematic frequency-sweep non-linearity on object distance estimation in FMCW/FSCW radar systems," in *33rd European Microwave Conference*, Oct 2003, pp. 1203–1206.

[2] M. Vossiek, P. Heide, M. Nalezinski, and V. Magori, "Novel FMCW radar system concept with adaptive compensation of phase errors," in *26th European Microwave Conference*, vol. 1, Sept 1996, pp. 135–139.

[3] H. Ahmed, A. Hafez, and A. Khalil, "Novel technique for reducing effects of non-linear frequency sweeps in LFM ranging radars," in *4th International Design and Test Workshop (IDT)*, Nov 2009, pp. 1–5.

[4] M. Girma, S. Beer, J. Hasch, M. Gonser, W. Debski, W. Winkler, Y. Sun, and T. Zwick, "Miniaturized 122 GHz system-in-package (SiP) short range radar sensor," in *10th European Radar Conference (EuRAD)*, Oct 2013, pp. 49–52.

[5] R. Feger, C. Pfeffer, W. Scheiblhofer, C. Schmid, M. Lang, and A. Stelzer, "A 77-ghz cooperative radar system based on multi-channel fmcw stations for local positioning applications," *Microwave Theory and Techniques, IEEE Transactions on*, vol. 61, no. 1, pp. 676–684, Jan 2013.

[6] A. Frischen, J. Hasch, and C. Waldschmidt, "Contour recognition with a cooperative distributed radar sensor network," in *International Conference on Microwaves for Intelligent Mobility (ICMIM)*, Apr 2015, pp. 1–4.

[7] ——, "Performance degradation in cooperative radar sensor systems due to uncorrelated phase noise," in *11th European Radar Conference (EuRAD)*, Oct 2014, pp. 241–244.